

Edge Information Hub-Empowered 6G NTN: Latency-Oriented Resource Orchestration and Configuration

Yueshan Lin, Wei Feng, *Senior Member, IEEE*, Yunfei Chen, *Senior Member, IEEE*, Ning Ge, *Member, IEEE*, Zhiyong Feng, *Senior Member, IEEE*, and Yue Gao, *Fellow, IEEE*

Abstract—Quick response to disasters is crucial for saving lives and reducing loss. This requires low-latency uploading of situation information to the remote command center. Since terrestrial infrastructures are often damaged in disaster areas, non-terrestrial networks (NTNs) are preferable to provide network coverage, and mobile edge computing (MEC) could be integrated to improve the latency performance. Nevertheless, the communications and computing in MEC-enabled NTNs are strongly coupled, which complicates the system design. In this paper, an edge information hub (EIH) that incorporates communication, computing and storage capabilities is proposed to synergize communication and computing and enable systematic design. We first address the joint data scheduling and resource orchestration problem to minimize the latency for uploading sensing data. The problem is solved using an optimal resource orchestration algorithm. On that basis, we propose the principles for resource configuration of the EIH considering payload constraints on size, weight and energy supply. Simulation results demonstrate the superiority of our proposed scheme in reducing the overall upload latency, thus enabling quick emergency rescue.

Index Terms—Edge information hub, latency, mobile edge computing, non-terrestrial network, resource orchestration.

I. INTRODUCTION

Every year, disasters (earthquakes, floods, fires, explosions, *etc.*) cause significant losses to both human lives and economies. To reduce such losses, immediate emergency responses and rescue operations are necessary. This requires real-time situation awareness of disaster areas [1]. For this purpose, a large amount of data collected by field sensors will be uploaded to the remote command center with low latency. The data are then analyzed for decision making and rescue operations [2]. Nevertheless, terrestrial communication infrastructures are often severely damaged in such disasters. Moreover, terrestrial networks might not cover areas where disasters take place, *e.g.*, forests and oceans [3]. Utilizing non-terrestrial networks (NTNs) such as satellites and unmanned aerial vehicles (UAVs) becomes crucial for disaster relief applications [4] [5].

Yueshan Lin, Wei Feng and Ning Ge are with the Department of Electronic Engineering, Tsinghua University, Beijing 100084, China (email: lins17@tsinghua.org.cn, fengwei@tsinghua.edu.cn, gening@tsinghua.edu.cn).

Yunfei Chen is with the Department of Engineering, University of Durham, Durham DH1 3LE, U.K. (e-mail: Yunfei.Chen@durham.ac.uk).

Zhiyong Feng is with the School of Information and Communication Engineering, Beijing University of Posts and Telecommunications, Beijing 100084, China (email:).

Yue Gao is with the School of Computer Science, Fudan University, Shanghai 200433, China (email: yue.gao@ieee.org).

In practice, collecting sensing data through NTNs also face inherent limitations. Both satellites and UAVs are usually limited by communication resources [6]. As the amount of data increases and the required latency decreases, a significant increase in the network throughput would be required, which may exceed the NTN's capability. Considering that the remote command center only requires key information on disaster areas to make rescue decisions, mobile edge computing (MEC) could be leveraged to process the sensing data and extract key information at the network edge [7]. In this way, only the extracted key information needs to be uploaded through the satellite backhaul, the burden of which could be significantly reduced to reduce overall latency.

In MEC-enabled NTNs, the communications and computing are strongly coupled. In this case, orchestrating the multi-dimensional network resources separately might result in low resource efficiency and unsatisfactory latency performance. Therefore, an edge information hub (EIH) that incorporates communications, computing and storage capabilities is proposed to synergize heterogeneous parts and enable systematic design. In practice, the EIH could be deployed on UAVs to empower the NTN. There are two major problems in the EIH-empowered NTN. First, the data scheduling and network resource orchestration need to be jointly optimized for synergy, where the network resources include communications, computing and storage resources. Besides, since UAVs usually have inherent limitations in size, weight and energy supply, it is necessary to derive the principles for resource configuration of the EIH. We thus focus on the optimal resource orchestration and the configuration for an EIH-Empowered NTN, which is envisioned a key part of the upcoming six-generation (6G) network.

A. Related Works

1) *Terrestrial Networks*: A number of terrestrial wireless solutions that support sensing data uploading as one of the Internet of Things (IoT) applications have been proposed. Some utilize the existing cellular networks for IoT applications, such as standards Extended Coverage GSM for IoT (EC-GSM-IoT) [8] and Category-M LTE specifications [9]. Others are based on low-power wide area network (LPWAN). The major technologies include Narrow-Band IoT (NB-IoT) [10] and Long Range Radio (LoRa) [11].

2) *Satellite Networks*: Since terrestrial networks are inherently limited by coverage, many existing studies consider

utilizing satellite-enabled NTN to provide services in remote and disaster areas. Sanctis *et al.* [12] introduced emergency management as well as two other application scenarios where satellite plays an important role. Specifically, satellites-enabled incident area networks could support both voice and data transmissions and wireless sensor and actuator communications in disaster areas. In [13], Centenaro *et al.* presented a survey on deployment solutions for exploiting satellites to provide IoT services where terrestrial networks are unavailable. In the survey they discussed the pros and cons of satellite access as far as IoT traffic is concerned. Fang *et al.* [14] proposed three basic models of satellite-enabled networks to support ubiquitous IoT applications. For each basic model, a survey of the state-of-the-art technologies was provided, and future research directions were discussed.

3) *Integrated Satellite-UAV Networks*: A number of existing studies further considered the integration of satellite and UAV networks for sensing data uploading. Bacco *et al.* [15] presented the design framework of a space information network (SIN) consisting of both satellites and UAVs to support IoT data exchanges. Examples of application scenarios as well as a possible relay solution were presented for the SIN. In [16], Zhu *et al.* formulated a two-level queuing network to model the two-tier networks with UAV access and GEO satellite backhaul. In this study, closed-form expressions for the network backlog and delay bounds were derived, and the access scale was optimized to obtain optimal network performance. Ma *et al.* [17] jointly optimized the trajectory of UAVs, the bandwidth allocation among users, the transmit powers of UAVs and the selections of LEO satellites, to increase the average achievable rate and uploaded data amount while decreasing the consumed energy. In [18], Liu *et al.* jointly optimized the subchannel allocation, the transmit power usage and the hovering times for data transmission efficiency maximization with a total latency constraint. The whole flight process of UAVs was considered for optimization and thus only the slowly-varying large-scale channel state information was used. Wang *et al.* [19] considered an integrated satellite-UAV framework where drones act as relays to upload the data from smart devices to low earth orbit satellites. They jointly optimized the smart devices connection scheduling, power control, and UAV trajectory to maximize the system capacity.

4) *MEC-enabled Integrated Satellite-UAV Networks*: To further reduce the latency, MEC servers could be utilized to compress the data at the network edge by removing redundant information. MEC-empowered NTN have been discussed in many studies. For instance, Lin *et al.* [20] proposed three minimal integrating structures of MEC and NTN, and established an on-demand network orchestration framework. In [21], Kim *et al.* investigated the data upload scheduling and path planning scheme for space-air-ground integrated edge computing systems, aimed at minimizing the total system energy cost. Ei *et al.* [22] determined the optimal data upload scheduling and bandwidth allocation to minimize the total latency. In [23], Chen *et al.* jointly optimized the upload scheduling proportion and computing resource allocation to minimize the system energy consumption under time delay

constraint. Chao *et al.* [24] considered maximizing the profit of the MEC service provider by jointly designing the upload scheduling decisions and the UAV positions. In [25], Waqar *et al.* jointly optimized the upload scheduling decision, the bandwidth allocation, the computation resource allocation and the power usage of users, to minimize the weighted sum of total time delay and energy consumption. Ding *et al.* [26] minimized the weighted sum energy consumption via joint user association, transmit precoding, task data assignment, and resource allocation. In [27], Hu *et al.* investigated the problem of joint optimization of the UAV 3D trajectory with resource allocation to maximizing the energy efficiency while satisfying users' quality-of-experience. Chai *et al.* [28] modelled the task data with dependencies as directed acyclic graphs and proposed a joint data upload scheduling and resource allocation scheme to improve the network efficiency. In [29], Liu *et al.* introduced a process-oriented framework that designs the whole process of data upload. Specifically, a latency minimization problem was formulated to optimize the data upload scheduling and power usage of users.

Although the studies mentioned above have made great progress in supporting sensing data uploading, there still exist research gaps. One is that the generalized optimal solution to the joint data scheduling and multi-dimensional resource orchestration problem has yet to be investigated. The existing studies discussed this problem by making assumptions to the system to simplify the problem and provide solutions for special cases. For instance, [22] proposed a joint data scheduling and subchannel allocation scheme assuming that the communication resources of the UAV-satellite link are equally allocated among users. In [29], it was assumed that the communication and computation procedures are conducted sequentially instead of concurrently to simplify the problem. In this case, the communication and computing resources may not be fully utilized in the data uploading procedure. Another research gap is that existing studies mainly focus on the orchestration of communication and computation resources, but have not considered how much resources should be configured in the network [23] [25] [27]. It should be noted that solving the resource configuration problem relies on optimally orchestrating the multi-dimensional resources. Therefore, it is necessary to jointly consider the resource configuration problem and the resource orchestration problem.

B. Main Contributions

In this paper, we consider the systematic design of an EIH-empowered NTN to support low-latency sensing data upload in disaster relief scenarios. We investigate the joint data scheduling, communication resource allocation and computing capability orchestration problem. An optimal joint data scheduling and resource orchestration scheme is proposed to minimize the overall latency. Based on the optimal resource orchestration scheme, we derive several principles for the resource configuration of the EIH. Simulation results are presented to verify the conclusions and demonstrate the superiority of the proposed scheme. The main contributions of this paper are summarized as follows.

- We model an EIH-empowered NTN to enable low-latency data uploading in disaster areas. In this model, the EIH is envisioned to synergize heterogeneous coupling parts, and enable systematic design. We formulate an overall upload latency minimization problem, where the data scheduling, the user-UAV transmission bandwidth allocation, the computing capability orchestration and the UAV-satellite data rate allocation are jointly considered.
- For the optimization problem, complicated piecewise functions exist in both the objective function and the constraints, rendering the problem hard to solve. We transform the problem by narrowing down its feasible region, and removing the piecewise functions. Accordingly, we equivalently recast the original problem into a convex form, and derive an optimal joint data scheduling and resource orchestration scheme.
- We derive the principles for resource configuration of the EIH, under its payload limitations in terms of size, weight and energy supply. Simulation results corroborate our theoretical achievements, and also demonstrate the superiority of our proposed scheme in reducing the overall upload latency.

The rest of this paper is organized as follows. In Section II, we introduce the system model of the EIH-empowered NTN. In Section III, we formulate the joint data scheduling and resource orchestration problem for latency minimization. We solve the problem and propose an optimal scheme in Section III. We further investigate the resource configuration problem and derive the principles for configuring the total computing capability in this section. Simulation results are presented in Section IV, while the conclusions of this paper are drawn in Section V.

II. SYSTEM MODEL

As shown in Fig. 1, we consider an EIH-empowered NTN, which consists of U users, a UAV equipped with an EIH, and a satellite to provide backhaul transmission. Each user u has sensing data of size D_u to upload. Fig. 2 presents the components of the EIH as well as the data flow diagram within it during the data upload process. The EIH incorporates a communication unit to the user, a communication unit to the satellite, a computing unit (*i.e.*, an MEC server) and a storage unit. During the data upload process, the EIH receives user u 's uploaded data through its communication module and store the data in its storage module. For user u , the data could be divided into two parts, namely to-be-computed data (ratio η_u) and to-be-uploaded data (ratio $1 - \eta_u$). The computing unit processes user u 's to-be-computed data with corresponding computing capability F_u (cycles/s), and returns the outcome to the storage unit as to-be-uploaded data. The computing intensity of user u 's data is denoted as ρ_u (cycles/bit). The computation could reduce the data size, where the computing output-to-input ratio is ζ_u . The to-be-uploaded data are transmitted to the satellite from the EIH, with the transmission rate R_u^S . It should be noted that all transmissions and computations mentioned above could proceed concurrently.

The communication model of user-UAV transmission is presented as follows. We assume that both the users and the

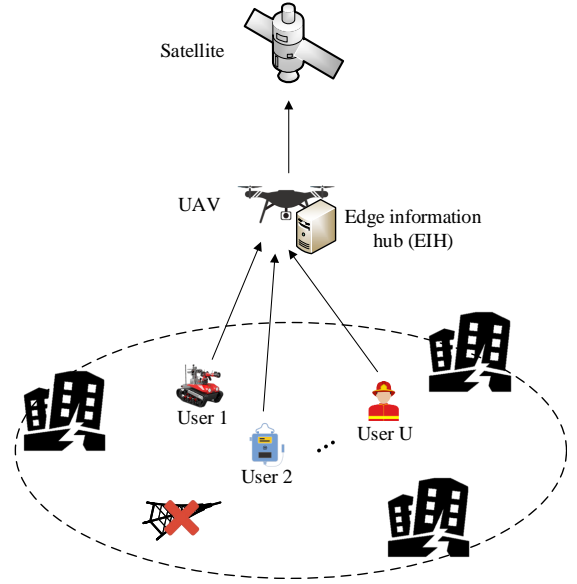


Fig. 1. Illustration of the EIH-based non-terrestrial network.

UAV have a single antenna, and therefore the received signal at the UAV from user u is given by

$$y_u = h_u x_u + n_u, \quad (1)$$

where x_u denotes the transmit signal, $n_u \sim \mathcal{CN}(0, \sigma^2)$ denotes the additive white Gaussian noise, and h_u denotes the channel between the user and the UAV, which can be modeled as

$$h_u = s \cdot l_u, \quad (2)$$

where s represents the fast-varying small-scale channel, which satisfies a complex Gaussian distribution with zero mean and unit variance (*i.e.*, Rayleigh fading), and l_u is the large-scale channel which can be expressed as follows [30].

$$l_u = 10^{-\frac{1}{20} \left(\frac{A_0}{1+a \exp(-b(\theta_u - a))} + B_0 \right)}, \quad (3)$$

where $A_0 = \eta_{\text{LoS}} - \eta_{\text{NLoS}}$ and $B_0 = \eta_{\text{NLoS}} + 20 \log_{10}(4\pi f d_u / c)$. In this model, η_{LoS} , η_{NLoS} , a and b are

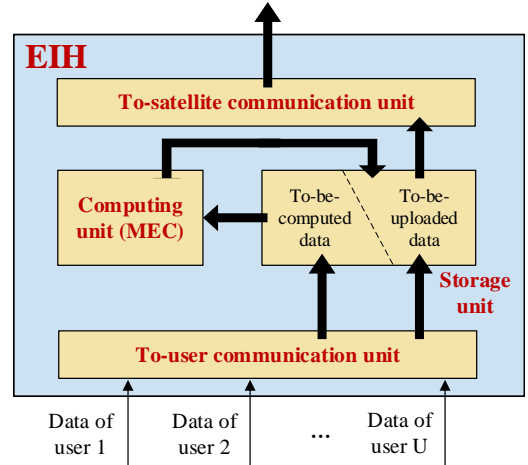


Fig. 2. Data flow diagram within the EIH during the sensing-data upload process.

$$T_u(B_u, R_u^S, F_u, \eta_u) = \begin{cases} \frac{D_u}{R_u^S}(\zeta_u \eta_u + 1 - \eta_u), & \eta_u B_u r_u \geq \frac{F_u}{\rho_u}, \frac{\zeta_u F_u}{\rho_u} + (1 - \eta_u) B_u r_u \geq R_u^S, \frac{F_u}{\rho_u} \geq \frac{\eta_u R_u^S}{\zeta_u \eta_u + 1 - \eta_u} & (5a) \\ \frac{\eta_u D_u \rho_u}{F_u}, & \eta_u B_u r_u \geq \frac{F_u}{\rho_u}, \frac{\zeta_u F_u}{\rho_u} + (1 - \eta_u) B_u r_u \geq R_u^S, \frac{F_u}{\rho_u} < \frac{\eta_u R_u^S}{\zeta_u \eta_u + 1 - \eta_u} & (5b) \\ \frac{\eta_u D_u \rho_u}{F_u}, & \eta_u B_u r_u \geq \frac{F_u}{\rho_u}, \frac{\zeta_u F_u}{\rho_u} + (1 - \eta_u) B_u r_u < R_u^S & (5c) \\ \frac{D_u}{R_u^S}(\zeta_u \eta_u + 1 - \eta_u), & \eta_u B_u r_u < \frac{F_u}{\rho_u}, (\zeta_u \eta_u + 1 - \eta_u) B_u r_u \geq R_u^S & (5d) \\ \frac{D_u}{B_u r_u}, & \eta_u B_u r_u < \frac{F_u}{\rho_u}, (\zeta_u \eta_u + 1 - \eta_u) B_u r_u < R_u^S & (5e) \end{cases}$$

$$V_u(B_u, R_u^S, F_u, \eta_u) = \begin{cases} \frac{D_u}{B_u r_u} \left[B_u r_u - R_u^S - (1 - \zeta_u) \frac{F_u}{\rho_u} \right], & \eta_u B_u r_u \geq \frac{F_u}{\rho_u}, \frac{\zeta_u F_u}{\rho_u} + (1 - \eta_u) B_u r_u \geq R_u^S, & \frac{F_u}{\rho_u} \geq \frac{\eta_u R_u^S}{\zeta_u \eta_u + 1 - \eta_u} & (6a) \\ \frac{D_u}{B_u r_u} \left[B_u r_u - R_u^S - (1 - \zeta_u) \frac{F_u}{\rho_u} \right], & \eta_u B_u r_u \geq \frac{F_u}{\rho_u}, \frac{\zeta_u F_u}{\rho_u} + (1 - \eta_u) B_u r_u \geq R_u^S, & \frac{F_u}{\rho_u} < \frac{\eta_u R_u^S}{\zeta_u \eta_u + 1 - \eta_u} & (6b) \\ \frac{D_u}{B_u r_u} \left(\eta_u B_u r_u - \frac{F_u}{\rho_u} \right), & \eta_u B_u r_u \geq \frac{F_u}{\rho_u}, \frac{\zeta_u F_u}{\rho_u} + (1 - \eta_u) B_u r_u < R_u^S & & (6c) \\ \frac{D_u}{B_u r_u} [(\zeta_u \eta_u + 1 - \eta_u) B_u r_u - R_u^S], & \eta_u B_u r_u < \frac{F_u}{\rho_u}, (\zeta_u \eta_u + 1 - \eta_u) B_u r_u \geq R_u^S & & (6d) \\ 0, & \eta_u B_u r_u < \frac{F_u}{\rho_u}, (\zeta_u \eta_u + 1 - \eta_u) B_u r_u < R_u^S & & (6e) \end{cases}$$

constants related to the propagation environment, d_u and θ_u are the distance and elevation angle between user u and the UAV respectively, f denotes the carrier frequency and c is the light speed. We assume that the users adopt a frequency division multiple access (FDMA) scheme to avoid interference. We use r_u to denote the ergodic spectrum efficiency, and the ergodic transmission rate can therefore be formulated as

$$R_u = B_u \mathbb{E} \left[\log_2 \left(1 + \frac{p_u |h_u|^2}{\sigma^2} \right) \right] = B_u r_u, \quad (4)$$

where B_u is the allocated bandwidth for user u , $p_u = \mathbb{E}(|x_u|^2)$ denotes the transmission power, and σ^2 denotes the noise power. We introduce a parameter r_u to denote the ergodic spectrum efficiency.

We use $T_u(B_u, R_u^S, F_u, \eta_u)$ to denote the total communication and computing latency for user u to upload its sensing data, and $V_u(B_u, R_u^S, F_u, \eta_u)$ to denote the minimum storage required by user u . Their specific expressions are shown in *Proposition 1*.

Proposition 1: The expression of $T_u(B_u, R_u^S, F_u, \eta_u)$ is given by (5), and the expression of $V_u(B_u, R_u^S, F_u, \eta_u)$ is given by (6) in the next page.

Proof 1: See Appendix A.

III. PROBLEM FORMULATION AND PROPOSED SCHEME

In this section, we formulate the joint data scheduling and resource orchestration problem for latency minimization and propose our solution to the problem. Specifically, we first obtain the optimal data scheduling variable. Then we transform the optimization problem by narrowing its feasible region, so that the complicated piecewise functions are simplified for a viable solution. Based on this solution, we further investigate the resource configuration problem and derive several principles for configuring the total computing capability.

A. Joint Data Scheduling and Resource Orchestration

We minimize the overall data upload latency by optimally determining each user's allocated bandwidth in the user-UAV transmission B_u , allocated data rate in the UAV-satellite transmission R_u^S , allocated computing resource F_u , as well as data scheduling η_u . The optimization problem can be formulated

TABLE I
OPTIMAL DATA SCHEDULING VARIABLE AND CORRESPONDING OPTIMIZED FUNCTION VALUES.

Condition	η_u^{opt}	$T_u^{\eta\text{-opt}}$	$V_u^{\eta\text{-opt}}$
$B_u r_u < R_u^S$	0	$\frac{D_u}{B_u r_u}$	0
$R_u^S \leq B_u r_u < \frac{R_u^S}{\zeta_u}, \frac{F_u}{\rho_u} < \frac{B_u r_u - R_u^S}{1 - \zeta_u}$	$\frac{F_u}{F_u(1 - \zeta_u) + \rho_u R_u^S}$	$\frac{D_u \rho_u}{F_u(1 - \zeta_u) + \rho_u R_u^S}$	$\frac{D_u}{B_u r_u} \left[B_u r_u - R_u^S - (1 - \zeta_u) \frac{F_u}{\rho_u} \right]$
$R_u^S \leq B_u r_u < \frac{R_u^S}{\zeta_u}, \frac{F_u}{\rho_u} \geq \frac{B_u r_u - R_u^S}{1 - \zeta_u}$	$\frac{B_u r_u - R_u^S}{(1 - \zeta_u) B_u r_u}$	$\frac{D_u}{B_u r_u}$	0
$B_u r_u \geq \frac{R_u^S}{\zeta_u}, \frac{F_u}{\rho_u} < \frac{R_u^S}{\zeta_u}$	$\frac{F_u}{F_u(1 - \zeta_u) + \rho_u R_u^S}$	$\frac{D_u \rho_u}{F_u(1 - \zeta_u) + \rho_u R_u^S}$	$\frac{D_u}{B_u r_u} \left[B_u r_u - R_u^S - (1 - \zeta_u) \frac{F_u}{\rho_u} \right]$
$B_u r_u \geq \frac{R_u^S}{\zeta_u}, \frac{R_u^S}{\zeta_u} \leq \frac{F_u}{\rho_u} < B_u r_u$	1	$\frac{\zeta_u D_u}{R_u^S}$	$\frac{D_u}{B_u r_u} \left[B_u r_u - R_u^S - (1 - \zeta_u) \frac{F_u}{\rho_u} \right]$
$B_u r_u \geq \frac{R_u^S}{\zeta_u}, \frac{F_u}{\rho_u} \geq B_u r_u$	1	$\frac{\zeta_u D_u}{R_u^S}$	$\frac{D_u}{B_u r_u} (\zeta_u B_u r_u - R_u^S)$

as

$$\min_{\mathbf{B}, \mathbf{R}^S, \mathbf{F}, \boldsymbol{\eta}} \max_u T_u(B_u, R_u^S, F_u, \eta_u) \quad (7a)$$

$$\text{s.t.} \quad \sum_{u=1}^U V_u(B_u, R_u^S, F_u, \eta_u) \leq V_{\text{total}}, \quad (7b)$$

$$\sum_{u=1}^U B_u \leq B_{\text{total}}, \quad (7c)$$

$$\sum_{u=1}^U R_u^S \leq R_{\text{total}}^S, \quad (7d)$$

$$\sum_{u=1}^U F_u \leq F_{\text{total}}, \quad (7e)$$

$$B_u \geq 0, \quad \forall u = 1, \dots, U, \quad (7f)$$

$$R_u^S \geq 0, \quad \forall u = 1, \dots, U, \quad (7g)$$

$$F_u \geq 0, \quad \forall u = 1, \dots, U, \quad (7h)$$

$$0 \leq \eta_u \leq 1, \quad \forall u = 1, \dots, U, \quad (7i)$$

where V_{total} , B_{total} , R_{total}^S , and F_{total} denote the total storage on UAV, the total bandwidth of user-UAV transmission, the total data rate of UAV-satellite transmission and the total computing capability of the computing unit, respectively. As shown in (5) and (6), both $T_u(B_u, R_u^S, F_u, \eta_u)$ and $V_u(B_u, R_u^S, F_u, \eta_u)$ are complicated piecewise functions, and thus problem (7) is difficult to solve.

B. Optimal Data Scheduling

By observing the expressions of $T_u(B_u, R_u^S, F_u, \eta_u)$ and $V_u(B_u, R_u^S, F_u, \eta_u)$ in (5) and (6), we present the following theorem

Theorem 1: Assume that the values of variables B_u , R_u^S and F_u are given, an optimal value of variable η_u^{opt} can be determined to minimize both functions $T_u(B_u, R_u^S, F_u, \eta_u)$ and $V_u(B_u, R_u^S, F_u, \eta_u)$. The expressions of η_u^{opt} and the corresponding minimized function values $T_u^{\eta\text{-opt}}(B_u, R_u^S, F_u) = T_u(B_u, R_u^S, F_u, \eta_u^{\text{opt}})$ and $V_u^{\eta\text{-opt}}(B_u, R_u^S, F_u) = V_u(B_u, R_u^S, F_u, \eta_u^{\text{opt}})$ are given in Table I.

Proof 2: See Appendix B.

Using Theorem 1, we present a new optimization problem (7) as

$$\min_{\mathbf{B}, \mathbf{R}^S, \mathbf{F}} \max_u T_u^{\eta\text{-opt}}(B_u, R_u^S, F_u) \quad (8a)$$

$$\text{s.t.} \quad \sum_{u=1}^U V_u^{\eta\text{-opt}}(B_u, R_u^S, F_u) \leq V_{\text{total}}, \quad (8b)$$

$$\sum_{u=1}^U B_u \leq B_{\text{total}}, \quad (8c)$$

$$\sum_{u=1}^U R_u^S \leq R_{\text{total}}^S, \quad (8d)$$

$$\sum_{u=1}^U F_u \leq F_{\text{total}}, \quad (8e)$$

$$B_u \geq 0, \quad \forall u = 1, \dots, U, \quad (8f)$$

$$R_u^S \geq 0, \quad \forall u = 1, \dots, U, \quad (8g)$$

$$F_u \geq 0, \quad \forall u = 1, \dots, U. \quad (8h)$$

The relationship between problem (7) and problem (8) is illustrated in the following theorem.

Theorem 2: The optimal objective functions in optimization problem (7) and optimization problem (8) are equal.

Proof 3: We adopt the method of proof by contradiction. Assume that the theorem does not hold. Since problem (8) has the same objective function as problem (7) but has a smaller feasible region, this is equivalent to the following statement. For problem (7) there exists at least one set of optimal variables $(\mathbf{B}_0, \mathbf{R}_0^S, \mathbf{F}_0, \boldsymbol{\eta}_0)$ lying outside the feasible region of problem (8), and satisfying that $\max_u T_u(B_{0,u}, R_{0,u}^S, F_{0,u}, \eta_{0,u}) < \max_u T_u^{\eta\text{-opt}}(B_u, R_u^S, F_u)$ holds for all feasible solutions $(\mathbf{B}, \mathbf{R}^S, \mathbf{F})$ of problem (8).

Consider $(\mathbf{B}_0, \mathbf{R}_0^S, \mathbf{F}_0)$ as a solution for problem (8). Obviously constraints (8c)-(8h) hold. For each $(B_{0,u}, R_{0,u}^S, F_{0,u})$ we obtain the corresponding η_u^{opt} according to Table I. There-

fore, we have

$$\begin{aligned} V_u^{\eta\text{-opt}}(B_{0,u}, R_{0,u}^S, F_{0,u}) &= V_u(B_{0,u}, R_{0,u}^S, F_{0,u}, \eta_u^{\text{opt}}) \\ &\leq V_u(B_{0,u}, R_{0,u}^S, F_{0,u}, \eta_{0,u}) \end{aligned} \quad (9)$$

This means that constraint (8b) also holds, and $(\mathbf{B}_0, \mathbf{R}_0^S, \mathbf{F}_0)$ is a feasible solution of problem (8). Besides, we have

$$\begin{aligned} T_u^{\eta\text{-opt}}(B_{0,u}, R_{0,u}^S, F_{0,u}) &= T_u(B_{0,u}, R_{0,u}^S, F_{0,u}, \eta_u^{\text{opt}}) \\ &\leq T_u(B_{0,u}, R_{0,u}^S, F_{0,u}, \eta_{0,u}) \end{aligned} \quad (10)$$

and thus the inequality $\max_u T_u(B_{0,u}, R_{0,u}^S, F_{0,u}, \eta_{0,u}) \geq \max_u T_u^{\eta\text{-opt}}(B_{0,u}, R_{0,u}^S, F_{0,u})$ holds, which causes contradiction. Therefore the assumption does not hold and the theorem is proved.

C. Optimal Resource Orchestration

Although we transform the problem equivalently, functions $T_u^{\eta\text{-opt}}(B_u, R_u^S, F_u)$ and $V_u^{\eta\text{-opt}}(B_u, R_u^S, F_u)$ are still complicated piecewise functions, which makes the problem hard to solve.

Based on problem (8), we present a new optimization problem as follows which further narrows down the feasible region so that both piecewise functions are simplified.

$$\min_{\mathbf{B}, \mathbf{R}^S, \mathbf{F}} \max_u \frac{D_u}{B_u r_u} \quad (11a)$$

$$\text{s.t.} \quad \sum_{u=1}^U B_u \leq B_{\text{total}}, \quad (11b)$$

$$\sum_{u=1}^U R_u^S \leq R_{\text{total}}^S, \quad (11c)$$

$$\sum_{u=1}^U F_u \leq F_{\text{total}}, \quad (11d)$$

$$R_u^S \leq B_u r_u \leq \frac{R_u^S}{\zeta_u}, \quad \forall u = 1, \dots, U, \quad (11e)$$

$$\frac{F_u}{\rho_u} = \frac{B_u r_u - R_u^S}{1 - \zeta_u}, \quad \forall u = 1, \dots, U, \quad (11f)$$

$$B_u \geq 0, \quad \forall u = 1, \dots, U, \quad (11g)$$

$$R_u^S \geq 0, \quad \forall u = 1, \dots, U, \quad (11h)$$

$$F_u \geq 0, \quad \forall u = 1, \dots, U. \quad (11i)$$

By introducing new constraints (11e) and (11f), according to the third row of Table I, both piecewise functions have a certain range, with expressions $T_u^{\eta\text{-opt}}(B_u, R_u^S, F_u) = \frac{D_u}{B_u r_u}$ and $V_u^{\eta\text{-opt}}(B_u, R_u^S, F_u) = 0$. Therefore the objective function (8a) changes into (11a), and constraint (8b) is removed in problem (11) since it always holds. The relationship between problem (8) and problem (11) is illustrated in the following theorem.

Theorem 3: The optimal objective functions in optimization problem (8) and optimization problem (11) are equal.

Proof 4: See Appendix C.

Finally, we introduce a slack variable T and equivalently recast the problem as

$$\min_{\mathbf{B}, \mathbf{R}^S, T} T \quad (12a)$$

$$\text{s.t.} \quad T \geq \frac{D_u}{B_u r_u}, \quad \forall u = 1, \dots, U, \quad (12b)$$

$$\sum_{u=1}^U B_u \leq B_{\text{total}}, \quad (12c)$$

$$\sum_{u=1}^U R_u^S \leq R_{\text{total}}^S, \quad (12d)$$

$$\sum_{u=1}^U \rho_u \frac{B_u r_u - R_u^S}{1 - \zeta_u} \leq F_{\text{total}}, \quad (12e)$$

$$R_u^S \leq B_u r_u \leq \frac{R_u^S}{\zeta_u}, \quad \forall u = 1, \dots, U, \quad (12f)$$

$$T \geq 0, \quad (12g)$$

$$B_u \geq 0, \quad \forall u = 1, \dots, U, \quad (12h)$$

$$R_u^S \geq 0, \quad \forall u = 1, \dots, U, \quad (12i)$$

It can be verified that problem (12) is a convex optimization problem and can be solved directly. We denote the optimal solution to this problem as $\bar{T}, \bar{\mathbf{B}} = [\bar{B}_1, \dots, \bar{B}_U], \bar{\mathbf{R}}^S = [\bar{R}_1^S, \dots, \bar{R}_U^S]$, where \bar{T} is the minimal overall data upload latency, and $\bar{\mathbf{B}}$ and $\bar{\mathbf{R}}^S$ are the optimal bandwidth allocation of user-UAV transmission and the optimal data rate allocation of UAV-satellite transmission, respectively. Moreover, the optimal computing capability orchestration $\bar{\mathbf{F}} = [\bar{F}_1, \dots, \bar{F}_U]$ can be given by

$$\bar{F}_u = \rho_u \frac{\bar{B}_u r_u - \bar{R}_u^S}{1 - \zeta_u}, \quad \forall u = 1, \dots, U, \quad (13)$$

and the optimal data scheduling variable could be obtained by substituting $\bar{\mathbf{B}}, \bar{\mathbf{R}}^S, \bar{\mathbf{F}}$ to calculate η^{opt} according to Table 1. By now, we have proposed the optimal joint data scheduling and resource orchestration scheme.

D. Resource Configuration

We further investigate the resource configuration problem based on the proposed data scheduling and resource allocation scheme. Specifically, we aim to obtain the relationship between the overall latency and the total configured resources $B_{\text{total}}, R_{\text{total}}^S$ and F_{total} . We present the following theorems

Theorem 4: Assume two optimization problems, both adopting the form of problem (12). For both problems, the corresponding parameters take the same values except for the total computing capability, where in the first problem it is $F_{\text{total}}^{(1)}$ while in the second it is $F_{\text{total}}^{(2)}$. If the following inequality holds

$$F_{\text{total}}^{(1)} \leq F_{\text{total}}^{(2)}, \quad (14)$$

then the optimal values of the objective functions of both problems, denoted as $\bar{T}^{(1)}$ and $\bar{T}^{(2)}$ respectively, satisfy

$$\bar{T}^{(1)} \geq \bar{T}^{(2)}. \quad (15)$$

Proof 5: Denote the optimal solution to the first and second problem as $(\bar{\mathbf{B}}^{(1)}, \bar{\mathbf{R}}^{S(1)}, \bar{T}^{(1)})$ and $(\bar{\mathbf{B}}^{(2)}, \bar{\mathbf{R}}^{S(2)}, \bar{T}^{(2)})$, respectively. Since $F_{\text{total}}^{(1)} \leq F_{\text{total}}^{(2)}$, $(\bar{\mathbf{B}}^{(1)}, \bar{\mathbf{R}}^{S(1)}, \bar{T}^{(1)})$ is also a feasible solution for the second problem, and because $(\bar{\mathbf{B}}^{(2)}, \bar{\mathbf{R}}^{S(2)}, \bar{T}^{(2)})$ is the optimal solution, the inequality $\bar{T}^{(1)} \geq \bar{T}^{(2)}$ holds, which proves the theorem.

Theorem 5: Define

$$F_{\text{total}}^{\text{lim}} = \left(\sum_{u=1}^U \rho_u D_u \right) \min \left\{ \frac{B_{\text{total}}}{\sum_{u=1}^U \frac{D_u}{r_u}}, \frac{R_{\text{total}}^S}{\sum_{u=1}^U \zeta_u D_u} \right\}, \quad (16)$$

and

$$T^{\text{lim}} = \max \left\{ \frac{\sum_{u=1}^U \frac{D_u}{r_u}}{B_{\text{total}}}, \frac{\sum_{u=1}^U \zeta_u D_u}{R_{\text{total}}^S} \right\}. \quad (17)$$

When the following inequality holds

$$F_{\text{total}} \geq F_{\text{total}}^{\text{lim}}, \quad (18)$$

the closed-form expressions of the optimal solution to problem (12) are given as

$$\bar{T} = T^{\text{lim}}, \quad (19)$$

$$\bar{B}_u = \frac{D_u}{r_u} \min \left\{ \frac{B_{\text{total}}}{\sum_{u=1}^U \frac{D_u}{r_u}}, \frac{R_{\text{total}}^S}{\sum_{u=1}^U \zeta_u D_u} \right\}, \quad \forall u = 1, \dots, U, \quad (20)$$

$$\bar{R}_u^S = \zeta_u D_u \min \left\{ \frac{B_{\text{total}}}{\sum_{u=1}^U \frac{D_u}{r_u}}, \frac{R_{\text{total}}^S}{\sum_{u=1}^U \zeta_u D_u} \right\}, \quad \forall u = 1, \dots, U. \quad (21)$$

Proof 6: See Appendix D.

Consider the following resource configuration problem: Given that the configured total user-UAV communication bandwidth B_{total} and total UAV-satellite data rate R_{total}^S are determined, to ensure that the minimized overall latency does not exceed a threshold T^{th} , how much total computing capability F_{total} needs to be configured?

Based on the Theorem 4 and Theorem 5 presented above, we propose the following resource configuration principles:

- If $T^{\text{th}} < T^{\text{lim}}$, it is impossible to finish the data upload within the threshold latency, no matter how much total computing capability F_{total} is configured.
- If $T^{\text{th}} \geq T^{\text{lim}}$, configuring the total computing capability as $F_{\text{total}} = F_{\text{total}}^{\text{lim}}$ is a sufficient condition to finish the data upload within the latency threshold, where T^{lim} is the corresponding overall latency. Further increasing F_{total} could not reduce the overall latency.

In the second scenario, the configuration scheme $F_{\text{total}} = F_{\text{total}}^{\text{lim}}$ is sufficient but probably not optimal, which could lead to resource redundancy. The optimal resource configuration problem is complicated and requires further research.

IV. SIMULATION RESULTS

We evaluate the performance of our proposed scheme through simulations in this section. The following simulation parameters are used unless otherwise specified. The number of users is set as $U = 4$. For each user's sensing data, the data size D_u is uniformly distributed in range $[\frac{1}{10}D_{\text{max}}, D_{\text{max}}]$, where the maximum data size is set as $D_{\text{max}} = 100$ Mbits. Besides, the computing intensity ρ_u is uniformly distributed in range $[1000, 5000]$ cycles/bit [31], and the computing output-to-input ratio is uniformly distributed in range $[0.01, 0.1]$ [32]. We assume that the position of the UAV is $[0, 0, 1000]^T$ m, and the users are uniformly distributed in a circle denoted as $\{[x, y, 0]^T | \sqrt{x^2 + y^2} \leq 1000(m)\}$. For the user-UAV transmission, the channel parameters are set as $(\eta_{\text{LoS}}, \eta_{\text{NLoS}}, a, b) = (0.1, 21, 5.0188, 0.3511)$ [33]. The carrier frequency f is set to be $f = 5.8$ GHz, and the speed of light is $c = 3 \times 10^8$ m/s. The transmit power for each user is set to be $p_u = 1$ W and the noise power is $\sigma^2 = -114$ dBm. The total bandwidth is set as $B_{\text{total}} = 0.5$ MHz. The ergodic spectrum efficiency between user u and the UAV r_u is obtained by averaging over 1000 generated small-scale channels. The total UAV-satellite transmission rate is set as $R_{\text{total}}^S = 0.5$ Mbits/s. Moreover, the total computing capability of the computing unit is set as $F_{\text{total}} = 5 \times 10^9$ cycles/s.

We first compare the proposed scheme with other different algorithms. A simple scheme is considered first where the UAV is not equipped with an MEC server. In addition to that, three other schemes are considered as

- Scheme 1: We consider the algorithm proposed in [29].
- Scheme 2: We consider a simplified version of our proposed algorithm, where we equally allocate the computing and communication resources to all users.
- Scheme 3: A simplified version of the algorithm proposed in [29] is used, where the computing and communication resources are allocated equally to all users.

In this simulation, we select a series of maximum data size D_{max} from 0.1 Mbits to 10 Mbits. The latency results are

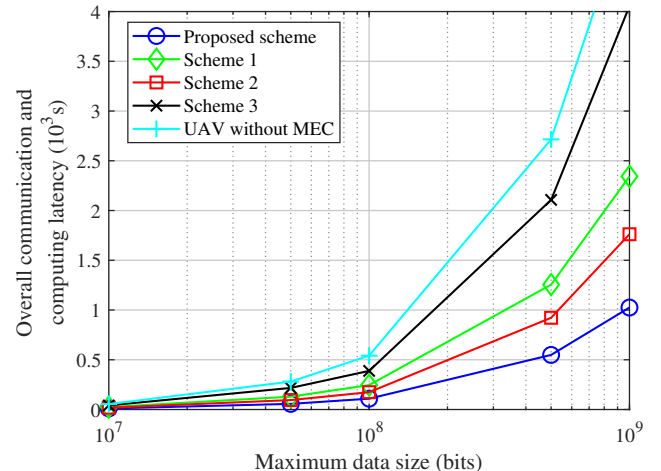


Fig. 3. Overall latency comparison among different algorithms with different maximum data size.

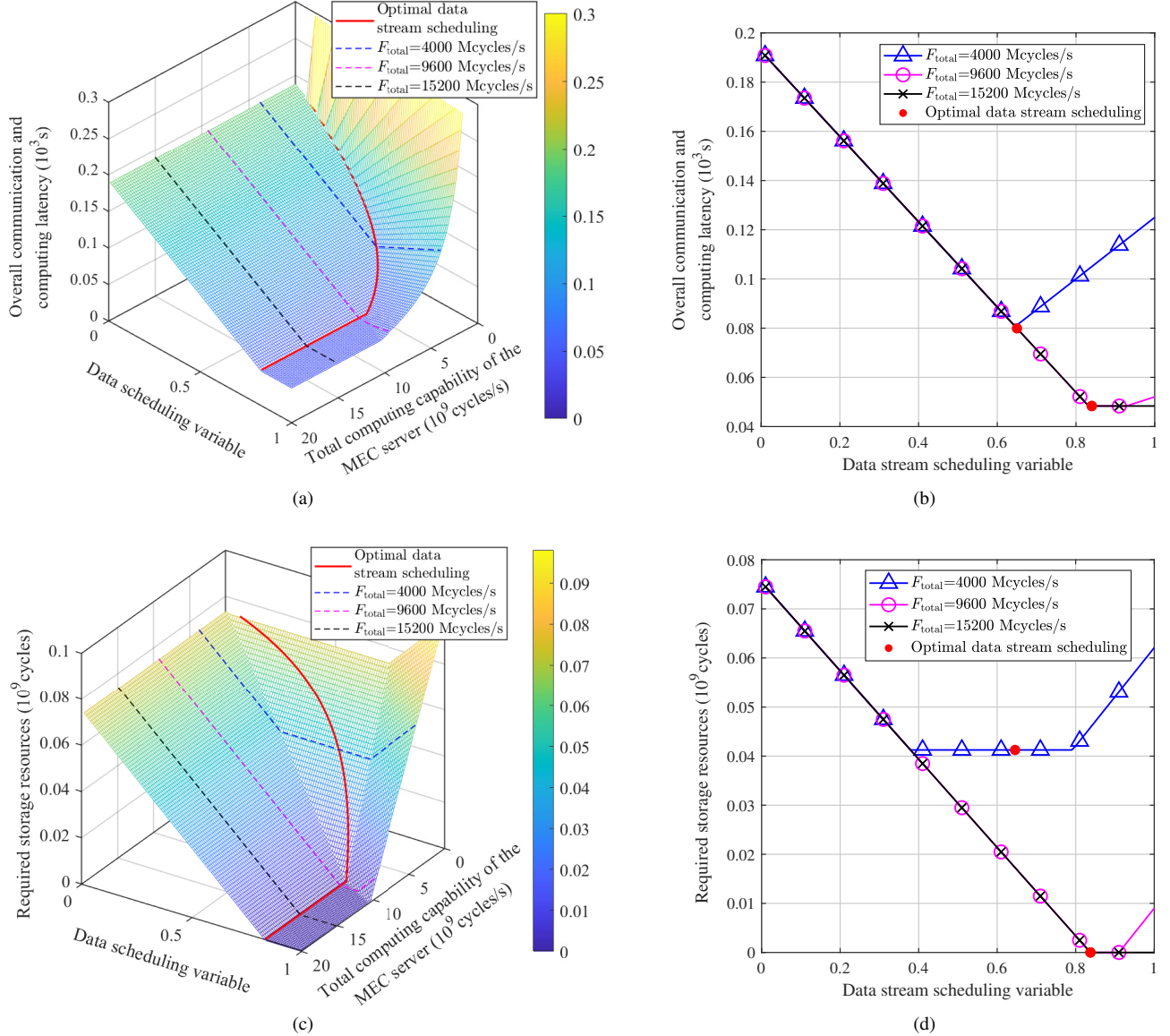


Fig. 4. Overall latency and the minimum storage required varying with the data scheduling variable.

averaged over 50 randomly-selected network topologies. As shown in Fig. 3, the proposed scheme could obtain better system performance than the scheme proposed in [29]. The reason is that in [29] the overall latency is the sum of the user-UAV transmission latency, the computing latency and the UAV-satellite transmission latency, while in our proposed scheme, the transmission and computing processes could be carried out simultaneously to decrease the overall latency. Also, by comparing the latency obtained by the proposed scheme and Scheme 2, one concludes that the resource orchestration optimization provides a significant performance gain in terms of upload latency.

In Fig. 4, we verify the performance of our proposed data scheduling scheme. Specifically, we consider the scenario of a single user, where both user-UAV bandwidth and UAV-satellite data rate are fixed ($B_{\text{total}} = 0.5$ MHz, $R_{\text{total}}^S = 0.5$ Mbits/s). With the total computing capability F_{total} varying

between $[0.2, 20] \times 10^9$ cycles/s, the relationship between the overall latency and the data scheduling variable is simulated, as shown in Fig. 4(a). The data scheduling variables obtained through our proposed method are also calculated and presented in Fig. 4(a). It can be observed that the data scheduling variable obtained by the proposed scheme always achieves the minimum latency at any given F_{total} . To show the results more clearly, we select three specific F_{total} values to sketch the overall latency with varying scheduling variables, as shown in Fig. 4(b). We can see that when F_{total} is relatively small, our proposed scheme obtains the exact optimal scheduling variable value to achieve the minimum latency. As F_{total} increases, variables in a certain interval are all optimal, and our proposed scheme always select a certain value in the interval. Similarly, Fig. 4(c) and Fig. 4(d) present the relationship between the required storage and the scheduling variable. We could also observe that our proposed scheme always obtain

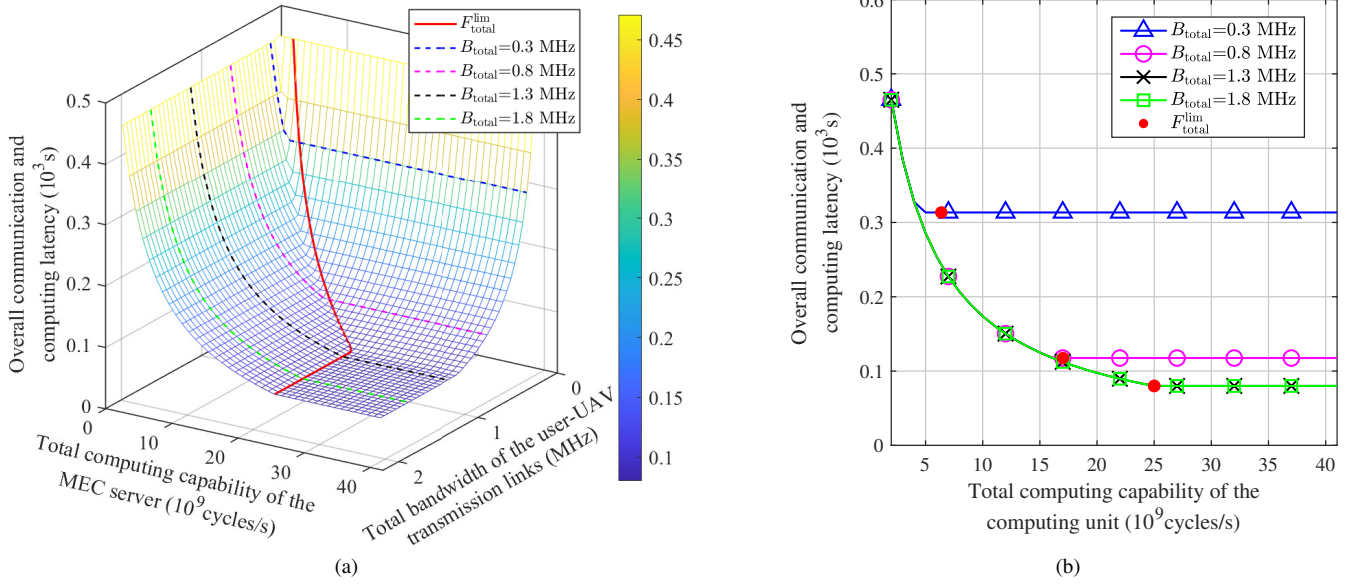


Fig. 5. Sufficient condition of the configured total computing capability and corresponding overall upload latency.

the scheduling variable that achieves the minimum required storage. We also notice that this minimized required storage appears to be 0, which means that if the data is properly scheduled, the system does not require extra storage resources for stranded data.

In Fig. 5, we verify the proposed principles for configuring the total computing capability. The total UAV-satellite data rate is set as $R_{total}^S = 0.5$ Mbits/s. As shown in Fig. 5(a), we depict the minimized overall latency obtained with varying user-UAV total bandwidth B_{total} and total computing capability F_{total} , as well as the latency obtained with F_{total}^{lim} . Four example values of B_{total} are selected to show the specific relationship in Fig. 5(b). We could see that for any given B_{total} , when F_{total} is larger than F_{total}^{lim} , the overall latency does not decline as F_{total} increases, which verifies our proposition. Besides, we notice from the $B_{total} = 0.3$ MHz scenario that the latency may stop declining before F_{total} reaches F_{total}^{lim} , which implies that further optimization of the configured total computing capability is possible. This requires further research into this problem.

Finally, in Fig. 6 we present the impact of the UAV-satellite total data rate R_{total}^S on the overall latency with varying user-UAV total transmission bandwidth B_{total} . The latency results are averaged over 50 randomly-selected network topologies. We can observe that as R_{total}^S increases the overall latency first reduces to a minimum and then remains unchanged. This is because when B_{total} is large enough the other two parameters become the system performance bottleneck. Besides, as R_{total}^S increases the overall latency decreases and eventually reaches a minimum value. Similarly, the reason is B_{total} becomes large enough and is no longer the bottleneck of the system performance.

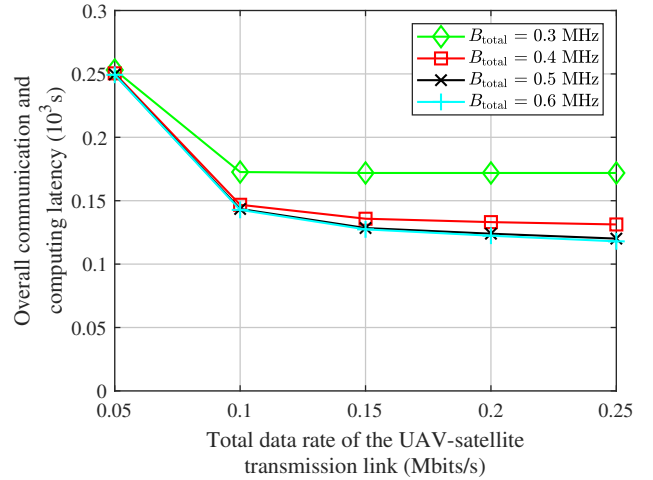


Fig. 6. Relationship between the overall latency and the UAV-satellite transmission bandwidth.

V. CONCLUSIONS

In this paper, we have modeled the EIH-empowered NTN to support low-latency sensing data upload for quick response to disasters. The EIH incorporates communications, computing and storage capabilities, which is envisioned to synergize heterogeneous coupling parts, and enable systematic design. We have investigated two major design problems of the EIH-empowered NTN to improve the latency performance and resource efficiency. First, the joint data scheduling and resource orchestration problem has been formulated for latency minimization. The problem has been transformed equivalently into a convex one. Thus, an optimal joint data scheduling and resource orchestration scheme has been proposed. On that basis, we have further derived the principles for resource

configuration of the EIH, under its payload limitations in terms of size, weight and energy supply. Simulation results have corroborated our theoretical achievements, and have also demonstrated the superiority of our proposed scheme in reducing the overall upload latency, thus enabling quick emergency rescue.

APPENDIX A PROOF OF Proposition 1

In order to obtain the expressions of the functions $T_u(B_u, R_u^S, F_u, \eta_u)$ and $V_u(B_u, R_u^S, F_u, \eta_u)$, we take the data flow perspective as shown in Fig. 2. We present five different situations based on the relationship among the data flow rates, and discuss the T_u and V_u expressions of each situation.

A. The amount of to-be-computed data and to-be-uploaded data in the storage both grow during the user-UAV transmission, and the former runs out first afterwards.

We first focus on the to-be-computed data in the storage unit as shown in Fig. 2. For this part of data, the input data flow is a ratio of the user-UAV transmitted data flow, with the data rate of $\eta_u B_u r_u$. Once the user-UAV transmission is completed, the input data rate becomes zero. The output data flow is the data flow to the computing unit for computation, which has data rate $\frac{F_u}{\rho_u}$. In the first situation, we assume

$$\eta_u B_u r_u \geq \frac{F_u}{\rho_u}, \quad (22)$$

which suggests that the amount of to-be-computed data in the storage grows during the user-UAV transmission.

Then we focus on the to-be-uploaded data in the storage unit. The input data flow for this part of data is a ratio of the user-UAV transmitted data flow plus the computed outcome data flow from the computing unit, and the combined data rate is $\frac{\zeta_u F_u}{\rho_u} + (1 - \eta_u) B_u r_u$. The input data rate also turns zero after the user-UAV transmission. The output data flow is the UAV-satellite transmitted data flow with the data rate of R_u^S . We assume in the first situation that

$$\frac{\zeta_u F_u}{\rho_u} + (1 - \eta_u) B_u r_u \geq R_u^S. \quad (23)$$

Similarly, this suggests that during the user-UAV transmission the amount of to-be-uploaded data in the storage unit grows.

The duration of user-UAV transmission could be calculated as $\frac{D_u}{B_u r_u}$. By the time the user-UAV transmission is completed, the to-be-computed data in the storage unit have the size of $\frac{D_u}{B_u r_u} (\eta_u B_u r_u - \frac{F_u}{\rho_u})$, and the size of the to-be-uploaded data is $\frac{D_u}{B_u r_u} [\frac{\zeta_u F_u}{\rho_u} + (1 - \eta_u) B_u r_u - R_u^S]$. We assume that the former part of data run out first after the user-UAV transmission is completed, which can be expressed as

$$\begin{aligned} & \frac{\frac{D_u}{B_u r_u} (\eta_u B_u r_u - \frac{F_u}{\rho_u})}{\frac{F_u}{\rho_u}} \\ & \leq \frac{\frac{D_u}{B_u r_u} [\frac{\zeta_u F_u}{\rho_u} + (1 - \eta_u) B_u r_u - R_u^S]}{R_u^S - \frac{\zeta_u F_u}{\rho_u}}, \end{aligned} \quad (24)$$

which can be further simplified as

$$\frac{F_u}{\rho_u} \geq \frac{\eta_u R_u^S}{\zeta_u \eta_u + 1 - \eta_u}. \quad (25)$$

Under these assumptions, the overall communication and computing latency is composed of three parts. The first part is the user-UAV transmission latency where data are accumulated in the storage. The second part is the latency of the to-be-computed data running out, and the third part is the latency of the remaining to-be-uploaded data running out. Therefore, the overall latency $T_u(B_u, R_u^S, F_u, \eta_u)$ can be expressed as

$$\begin{aligned} T_u &= \frac{D_u}{B_u r_u} + \frac{\frac{D_u}{B_u r_u} (\eta_u B_u r_u - \frac{F_u}{\rho_u})}{\frac{F_u}{\rho_u}} \\ &+ \frac{1}{R_u^S} \left\{ \frac{D_u}{B_u r_u} \left[\frac{\zeta_u F_u}{\rho_u} + (1 - \eta_u) B_u r_u - R_u^S \right] \right. \\ &\quad \left. - (R_u^S - \frac{\zeta_u F_u}{\rho_u}) \frac{\frac{D_u}{B_u r_u} (\eta_u B_u r_u - \frac{F_u}{\rho_u})}{\frac{F_u}{\rho_u}} \right\} \\ &= \frac{D_u}{R_u^S} (\zeta_u \eta_u + 1 - \eta_u). \end{aligned} \quad (26)$$

This expression can be understood in a simpler way, namely the UAV-satellite transmission data rate is the bottleneck of the system, and thus the overall latency is the total data to be transmitted from the UAV to the satellite $D_u (\zeta_u \eta_u + 1 - \eta_u)$ divided by the UAV-satellite transmission rate R_u^S .

We further consider the minimum storage $V_u(B_u, R_u^S, F_u, \eta_u)$ required. It can be observed that the storage unit accumulates data during the user-UAV transmission, and afterwards the amount of data decreases because of the computation and transmission to the satellite. Therefore, the minimum storage $V_u(B_u, R_u^S, F_u, \eta_u)$ required corresponds to the moment at which the user-UAV transmission is just completed, and the expression is

$$V_u = \frac{D_u}{B_u r_u} \left[B_u r_u - R_u^S - (1 - \zeta_u) \frac{F_u}{\rho_u} \right]. \quad (27)$$

In this first situation, we prove that under assumptions (22), (23) and (25), the expressions for $T_u(B_u, R_u^S, F_u, \eta_u)$ and $V_u(B_u, R_u^S, F_u, \eta_u)$ are shown in (26) and (27), which corresponds to (5a) and (6a).

B. The amount of to-be-computed data and to-be-uploaded data in the storage both grow during the user-UAV transmission, and the latter runs out first afterwards.

In the second situation, we assume that (22) and (23) still hold. This means that during the user-UAV transmission, both the to-be-computed data and the to-be-uploaded data are accumulating in the storage unit.

Different from the first situation, we assume that the to-be-uploaded data to the satellite in the storage run out first, which means that the following inequality holds

$$\frac{F_u}{\rho_u} < \frac{\eta_u R_u^S}{\zeta_u \eta_u + 1 - \eta_u}. \quad (28)$$

Under the assumptions (22), (23) and (28), the overall communication and computing latency include the latency of

user-UAV transmission and the latency of the to-be-computed data running out in the storage. In this case, the expression of $T_u(B_u, R_u^S, F_u, \eta_u)$ is given by

$$\begin{aligned} T_u &= \frac{D_u}{B_u r_u} + \frac{\frac{D_u}{B_u r_u}(\eta_u B_u r_u - \frac{F_u}{\rho_u})}{\frac{F_u}{\rho_u}} \\ &= \frac{\eta_u D_u \rho_u}{F_u}. \end{aligned} \quad (29)$$

This expression shows that the computation capability is the bottleneck of this system, and the overall latency is the total data required to be computed $\eta_u D_u$ divided by the computing unit throughput F_u/ρ_u .

Similar to the first situation, the data in the storage unit achieve maximum amount at the moment when the user-UAV transmission is completed, and therefore the expression of the minimum storage required $V_u(B_u, R_u^S, F_u, \eta_u)$ in this situation is the same as (27).

We prove that in the second situation, under assumptions (22), (23) and (28), the expressions for $T_u(B_u, R_u^S, F_u, \eta_u)$ and $V_u(B_u, R_u^S, F_u, \eta_u)$ are shown as in (29) and (27), which corresponds to (5b) and (6b).

C. Only the amount of to-be-computed data in the storage grow during the user-UAV transmission.

In the third situation, we assume that inequality (22) still holds, which means that the amount of to-be-computed data are increasing during the user-UAV transmission.

Nevertheless, we assume that instead of (23), the following inequality holds in this situation

$$\frac{\zeta_u F_u}{\rho_u} + (1 - \eta_u) B_u r_u < R_u^S, \quad (30)$$

which means that the output data rate is larger than the input data rate for the part of to-be-uploaded data in the storage unit. In this case, the actual UAV-satellite data rate (output data rate) is the same as the partial user-UAV transmitted data rate and the computed outcome data rate combined (input data rate) during the user-UAV transmission. Afterwards the actual UAV-satellite data rate becomes the same as the computed outcome data rate. The amount of to-be-uploaded data to the satellite in the storage unit is always equal to zero in this situation.

Similar to the second situation, the computation rate is the bottleneck of the system since the whole process is finished when the to-be-computed data in the storage run out. The expression of $T_u(B_u, R_u^S, F_u, \eta_u)$ is the same as (29).

Maximum data amount in the storage is achieved when the user-UAV transmission is just finished, and the required storage size $T_u(B_u, R_u^S, F_u, \eta_u)$ can be given by

$$V_u = \frac{D_u}{B_u r_u} \left(\eta_u B_u r_u - \frac{F_u}{\rho_u} \right). \quad (31)$$

The minimum required storage in this situation is different from the previous two situations because the actual UAV-satellite data rate changes to match the input data rate of the to-be-uploaded data in the storage.

In this subsection, we prove that in the third situation, under assumptions (22) and (30), the expressions for

$T_u(B_u, R_u^S, F_u, \eta_u)$ and $V_u(B_u, R_u^S, F_u, \eta_u)$ are shown as in (29) and (31), which corresponds to (5c) and (6c).

D. Only the amount of to-be-uploaded data in the storage grow during the user-UAV transmission.

We assume in the fourth situation that the following inequality instead of (22) holds

$$\eta_u B_u r_u < \frac{F_u}{\rho_u}, \quad (32)$$

which means that the output data rate is larger than the input data rate for the to-be-computed data in the storage unit. In this case, the actual data rate of the computing unit obtaining data from the storage (output data rate) is the same as the partial user-UAV transmitted data rate (input data rate) during the user-UAV transmission. The amount of to-be-computed data in the storage always equals to zero.

We also assume that the following inequality holds

$$(\zeta_u \eta_u + 1 - \eta_u) B_u r_u \geq R_u^S, \quad (33)$$

which means the input data rate for the to-be-uploaded data in the storage unit is larger than the output data rate and the data amount is growing during the user-UAV transmission. It should be noted that (33) is different from (23) because the computing unit throughput changes in this situation.

Because the whole process ends when the to-be-uploaded data in the storage unit run out, the system is limited by the UAV-satellite transmission rate, and the overall communication and computation latency $T_u(B_u, R_u^S, F_u, \eta_u)$ is the same as (26).

The data amount in the storage also reaches the maximum value when the user-UAV transmission is just finished, and the minimum storage required $V_u(B_u, R_u^S, F_u, \eta_u)$ can be given by

$$V_u = \frac{D_u}{B_u r_u} [(\zeta_u \eta_u + 1 - \eta_u) B_u r_u - R_u^S]. \quad (34)$$

In the fourth situation, we prove that under assumptions (32) and (33), the expressions for $T_u(B_u, R_u^S, F_u, \eta_u)$ and $V_u(B_u, R_u^S, F_u, \eta_u)$ are shown as in (26) and (34), which corresponds to (5d) and (6d).

E. Neither the amount of to-be-computed data nor the amount of to-be-uploaded data in the storage grow during the user-UAV transmission.

In the fifth situation, we assume that (32) still holds which suggests that the amount of to-be-computed data in the storage unit is always zero.

We also assume that the following inequality instead of (33) holds

$$(\zeta_u \eta_u + 1 - \eta_u) B_u r_u < R_u^S, \quad (35)$$

which means the input data rate for the to-be-uploaded data in the storage unit is smaller than the output data rate. In this case the amount of the to-be-uploaded data in the storage also always equals zero.

In this situation, no amount of data are accumulating in the storage. Thus, the whole process is finished when the user-UAV transmission is completed, and the overall communication and computation latency $T_u(B_u, R_u^S, F_u, \eta_u)$ is

$$T_u = \frac{D_u}{B_u r_u}, \quad (36)$$

and the minimum required storage $V_u(B_u, R_u^S, F_u, \eta_u)$ is

$$V_u = 0. \quad (37)$$

We prove that under assumptions (32) and (35), the expressions for $T_u(B_u, R_u^S, F_u, \eta_u)$ and $V_u(B_u, R_u^S, F_u, \eta_u)$ are shown as in (36) and (37), which corresponds to (5e) and (6e).

APPENDIX B PROOF OF *Theorem 1*

Assuming that the values of variables B_u , R_u^S and F_u are given, we present three different situations based on the relationship between B_u and R_u^S . The optimal value of variable η_u^{opt} and the corresponding minimized function values $T_u^{\eta\text{-opt}}(B_u, R_u^S, F_u) = T_u(B_u, R_u^S, F_u, \eta_u^{\text{opt}})$ and $V_u^{\eta\text{-opt}}(B_u, R_u^S, F_u) = V_u(B_u, R_u^S, F_u, \eta_u^{\text{opt}})$ are discussed in each situation.

A. $B_u r_u < R_u^S$

Under this assumption, we further discuss the relationship between T_u and η_u and the relationship between V_u and η_u given different F_u values.

We first assume

$$\frac{F_u}{\rho_u} < B_u r_u. \quad (38)$$

In this case, when the following inequality holds

$$0 \leq \eta_u < \frac{F_u}{\rho_u B_u r_u}, \quad (39)$$

the expressions of T_u and V_u refer to (5e) and (6e), where T_u and V_u remain unchanged with η_u increasing. Besides, when the following inequality holds

$$\frac{F_u}{\rho_u B_u r_u} \leq \eta_u \leq 1, \quad (40)$$

the expressions of T_u and V_u refer to (5c) and (6c), where both T_u and V_u monotonically increase with η_u increasing. Therefore, the optimal η_u could be arbitrarily taken in the range of $[0, \frac{F_u}{\rho_u B_u r_u})$.

Then we assume

$$\frac{F_u}{\rho_u} \geq B_u r_u. \quad (41)$$

In this case, for

$$0 \leq \eta_u \leq 1, \quad (42)$$

the expressions of T_u and V_u refer to (5e) and (6e), where T_u and V_u remain unchanged with η_u increasing. Therefore, the optimal η_u could be arbitrarily taken in the range of $[0, 1]$.

Therefore, on the condition of

$$B_u r_u < R_u^S, \quad (43)$$

we set the optimal value of η_u to be

$$\eta_u^{\text{opt}} = 0, \quad (44)$$

for the simplicity of expression. The corresponding function values are

$$T_u^{\eta\text{-opt}}(B_u, R_u^S, F_u) = \frac{D_u}{B_u r_u}, \quad (45)$$

$$V_u^{\eta\text{-opt}}(B_u, R_u^S, F_u) = 0. \quad (46)$$

This verifies the first row of Table I.

B. $R_u^S \leq B_u r_u < \frac{R_u^S}{\zeta_u}$

we also discuss the relationship between T_u and η_u and the relationship between V_u and η_u given different F_u values as follows.

We first assume

$$\frac{F_u}{\rho_u} < \frac{B_u r_u - R_u^S}{1 - \zeta_u}. \quad (47)$$

In this case, when the following inequality holds

$$0 \leq \eta_u < \frac{F_u}{\rho_u B_u r_u}, \quad (48)$$

the expressions of T_u and V_u refer to (5d) and (6d), where both T_u and V_u monotonically decrease with η_u increasing. When the following inequality holds

$$\frac{F_u}{\rho_u B_u r_u} \leq \eta_u < \frac{F_u}{\rho_u R_u^S + (1 - \zeta_u) F_u}, \quad (49)$$

the expressions of T_u and V_u refer to (5a) and (6a), and with η_u increasing, T_u monotonically decrease while V_u remain unchanged. When the following inequality holds

$$\begin{aligned} \frac{F_u}{\rho_u R_u^S + (1 - \zeta_u) F_u} &\leq \eta_u \\ &< \frac{\rho_u (B_u r_u - R_u^S) + \zeta_u F_u}{\rho_u B_u r_u}, \end{aligned} \quad (50)$$

the expressions of T_u and V_u refer to (5b) and (6b), and with η_u increasing, T_u monotonically increase while V_u remain unchanged. Finally, when the following inequality holds

$$\frac{\rho_u (B_u r_u - R_u^S) + \zeta_u F_u}{\rho_u B_u r_u} \leq \eta_u \leq 1, \quad (51)$$

the expressions of T_u and V_u refer to (5c) and (6c), where both T_u and V_u monotonically increase with η_u increasing. Therefore, on the condition of

$$R_u^S \leq B_u r_u < \frac{R_u^S}{\zeta_u}, \quad \frac{F_u}{\rho_u} < \frac{B_u r_u - R_u^S}{1 - \zeta_u} \quad (52)$$

the optimal value of η_u to minimize both functions is determined to be

$$\eta_u^{\text{opt}} = \frac{F_u}{\rho_u R_u^S + (1 - \zeta_u) F_u}, \quad (53)$$

and the corresponding function values are

$$T_u^{\eta\text{-opt}}(B_u, R_u^S, F_u) = \frac{\rho_u D_u}{\rho_u R_u^S + (1 - \zeta_u) F_u}, \quad (54)$$

$$V_u^{\eta\text{-opt}}(B_u, R_u^S, F_u) = \frac{D_u}{B_u r_u} \left[B_u r_u - R_u^S - (1 - \zeta_u) \frac{F_u}{\rho_u} \right], \quad (55)$$

This verifies the second row of Table I.

Then we assume

$$\frac{B_u r_u - R_u^S}{1 - \zeta_u} \leq \frac{F_u}{\rho_u} < B_u r_u. \quad (56)$$

In this case, when the following inequality holds

$$0 \leq \eta_u < \frac{B_u r_u - R_u^S}{(1 - \zeta_u) B_u r_u}, \quad (57)$$

the expressions of T_u and V_u refer to (5d) and (6d), where both T_u and V_u monotonically decrease with η_u increasing. When the following inequality holds

$$\frac{B_u r_u - R_u^S}{(1 - \zeta_u) B_u r_u} \leq \eta_u < \frac{F_u}{\rho_u B_u r_u}, \quad (58)$$

the expressions of T_u and V_u refer to (5e) and (6e), where T_u and V_u remain unchanged with η_u increasing. When the following inequality holds

$$\frac{F_u}{\rho_u B_u r_u} \leq \eta_u \leq 1, \quad (59)$$

the expressions of T_u and V_u refer to (5c) and (6c), where both T_u and V_u monotonically increase with η_u increasing. Therefore, the optimal η_u could be arbitrarily taken in the range of $[\frac{B_u r_u - R_u^S}{(1 - \zeta_u) B_u r_u}, \frac{F_u}{\rho_u B_u r_u})$.

Finally we assume

$$\frac{F_u}{\rho_u} \geq B_u r_u. \quad (60)$$

In this case, when the following inequality holds

$$0 \leq \eta_u < \frac{B_u r_u - R_u^S}{(1 - \zeta_u) B_u r_u}, \quad (61)$$

the expressions of T_u and V_u refer to (5d) and (6d), where both T_u and V_u monotonically decrease with η_u increasing. When the following inequality

$$\frac{B_u r_u - R_u^S}{(1 - \zeta_u) B_u r_u} \leq \eta_u \leq 1, \quad (62)$$

the expressions of T_u and V_u refer to (5e) and (6e), where T_u and V_u remain unchanged with η_u increasing. Therefore, the optimal η_u could be arbitrarily taken in the range of $[\frac{B_u r_u - R_u^S}{(1 - \zeta_u) B_u r_u}, 1]$.

Therefore, on the condition of

$$R_u^S \leq B_u r_u < \frac{R_u^S}{\zeta_u}, \frac{F_u}{\rho_u} \geq \frac{B_u r_u - R_u^S}{1 - \zeta_u}, \quad (63)$$

we set the optimal value of η_u to be

$$\eta_u^{\text{opt}} = \frac{B_u r_u - R_u^S}{(1 - \zeta_u) B_u r_u}, \quad (64)$$

for the simplicity of expression. The corresponding function values are

$$T_u^{\eta\text{-opt}}(B_u, R_u^S, F_u) = \frac{D_u}{B_u r_u}, \quad (65)$$

$$V_u^{\eta\text{-opt}}(B_u, R_u^S, F_u) = 0. \quad (66)$$

This verifies the third row of Table I.

C. $B_u r_u \geq \frac{R_u^S}{\zeta_u}$

We first assume

$$\frac{F_u}{\rho_u} < \frac{R_u^S}{\zeta_u}. \quad (67)$$

In this case, when the following inequality holds

$$0 \leq \eta_u < \frac{F_u}{\rho_u B_u r_u}, \quad (68)$$

the expressions of T_u and V_u refer to (5d) and (6d), where both T_u and V_u monotonically decrease with η_u increasing. When the following inequality holds

$$\frac{F_u}{\rho_u B_u r_u} \leq \eta_u < \frac{F_u}{\rho_u R_u^S + (1 - \zeta_u) F_u}, \quad (69)$$

the expressions of T_u and V_u refer to (5a) and (6a), and with η_u increasing, T_u monotonically decrease while V_u remain unchanged. When the following inequality holds

$$\begin{aligned} \frac{F_u}{\rho_u R_u^S + (1 - \zeta_u) F_u} &\leq \eta_u \\ &< \frac{\rho_u (B_u r_u - R_u^S) + \zeta_u F_u}{\rho_u B_u r_u}, \end{aligned} \quad (70)$$

the expressions of T_u and V_u refer to (5b) and (6b). With η_u increasing, T_u monotonically increase while V_u remain unchanged. Finally, when the following inequality holds

$$\frac{\rho_u (B_u r_u - R_u^S) + \zeta_u F_u}{\rho_u B_u r_u} \leq \eta_u \leq 1, \quad (71)$$

the expressions of T_u and V_u refer to (5c) and (6c), where both T_u and V_u monotonically increase with η_u increasing. Therefore, on the condition of

$$B_u r_u \geq \frac{R_u^S}{\zeta_u}, \frac{F_u}{\rho_u} < \frac{R_u^S}{\zeta_u}, \quad (72)$$

the optimal value of η_u to minimize both functions is determined to be

$$\eta_u^{\text{opt}} = \frac{F_u}{\rho_u R_u^S + (1 - \zeta_u) F_u}, \quad (73)$$

and the corresponding function values are

$$T_u^{\eta\text{-opt}}(B_u, R_u^S, F_u) = \frac{\rho_u D_u}{\rho_u R_u^S + (1 - \zeta_u) F_u}, \quad (74)$$

$$V_u^{\eta\text{-opt}}(B_u, R_u^S, F_u) = \frac{D_u}{B_u r_u} \left[B_u r_u - R_u^S - (1 - \zeta_u) \frac{F_u}{\rho_u} \right]. \quad (75)$$

This verifies the fourth row of Table I.

We then assume

$$\frac{R_u^S}{\zeta_u} \leq \frac{F_u}{\rho_u} < B_u r_u. \quad (76)$$

In this case, when the following inequality holds

$$0 \leq \eta_u < \frac{F_u}{\rho_u B_u r_u}, \quad (77)$$

the expressions of T_u and V_u refer to (5d) and (6d), where both T_u and V_u monotonically decrease with η_u increasing. When the following inequality holds

$$\frac{F_u}{\rho_u B_u r_u} \leq \eta_u \leq 1, \quad (78)$$

the expressions of T_u and V_u refer to (5a) and (6a). With η_u increasing, T_u monotonically decrease while V_u remain unchanged. Therefore, on the condition of

$$B_u r_u \geq \frac{R_u^S}{\zeta_u}, \quad \frac{R_u^S}{\zeta_u} \leq \frac{F_u}{\rho_u} < B_u r_u, \quad (79)$$

the optimal value of η_u to minimize both functions is determined to be

$$\eta_u^{\text{opt}} = 1, \quad (80)$$

and the corresponding function values are

$$T_u^{\eta\text{-opt}}(B_u, R_u^S, F_u) = \frac{\zeta_u D_u}{R_u^S}, \quad (81)$$

$$V_u^{\eta\text{-opt}}(B_u, R_u^S, F_u) = \frac{D_u}{B_u r_u} [B_u r_u - R_u^S - (1 - \zeta_u) \frac{F_u}{\rho_u}]. \quad (82)$$

This verifies the fifth row of Table I.

Finally we assume

$$\frac{F_u}{\rho_u} \geq B_u r_u. \quad (83)$$

In this case, for

$$0 \leq \eta_u \leq 1 \quad (84)$$

the expressions of T_u and V_u refer to (5d) and (6d), where both T_u and V_u monotonically decrease with η_u increasing. Therefore, on the condition of

$$B_u r_u \geq \frac{R_u^S}{\zeta_u}, \quad \frac{F_u}{\rho_u} \geq B_u r_u, \quad (85)$$

the optimal value of η_u to minimize both functions is determined to be

$$\eta_u^{\text{opt}} = 1, \quad (86)$$

and the corresponding function values are

$$T_u^{\eta\text{-opt}}(B_u, R_u^S, F_u) = \frac{\zeta_u D_u}{R_u^S}, \quad (87)$$

$$V_u^{\eta\text{-opt}}(B_u, R_u^S, F_u) = \frac{D_u}{B_u r_u} (\zeta_u B_u r_u - R_u^S). \quad (88)$$

This verifies the sixth row of Table I.

APPENDIX C PROOF OF *Theorem 3*

We refer to the proof of *Theorem 2* and also adopt the method of proof by contradiction. Assume that the theorem does not hold, which is equivalent to the following statement. For problem (8) there exists at least one set of optimal variables $(\mathbf{B}_0, \mathbf{R}_0^S, \mathbf{F}_0)$ lying outside the feasible region of problem (11), and satisfying that

$$\max_u T_u^{\eta\text{-opt}}(B_{0,u}, R_{0,u}^S, F_{0,u}) < \max_u \frac{D_u}{B_u r_u} \quad (89)$$

holds for all feasible solutions $(\mathbf{B}, \mathbf{R}^S, \mathbf{F})$ of problem (11). We categorize the elements of $(\mathbf{B}_0, \mathbf{R}_0^S, \mathbf{F}_0)$ based on the relationship among $B_{0,u}$, $R_{0,u}^S$ and $F_{0,u}$.

Select all elements from $(\mathbf{B}_0, \mathbf{R}_0^S, \mathbf{F}_0)$ that satisfy

$$B_{0,u} r_u < R_{0,u}^S, \quad (90)$$

corresponding to the first row of Table I. For any one of those elements $(B_{0,u}, R_{0,u}^S, F_{0,u})$, we present a corresponding solution $(B_{1,u}, R_{1,u}^S, F_{1,u})$ which satisfies

$$\begin{cases} B_{1,u} = B_{0,u} & (91a) \\ R_{1,u}^S = B_{0,u} r_u & (91b) \\ F_{1,u} = 0 & (91c) \end{cases}$$

We can first verify that

$$(B_{1,u}, R_{1,u}^S, F_{1,u}) \leq (B_{0,u}, R_{0,u}^S, F_{0,u}) \quad (92)$$

holds. Besides, we can verify that

$$R_{1,u}^S \leq B_{1,u} r_u \leq \frac{R_{1,u}^S}{\zeta_u} \quad (93)$$

and

$$\frac{F_{1,u}}{\rho_u} = \frac{B_{1,u} r_u - R_{1,u}^S}{1 - \zeta_u} \quad (94)$$

also hold. Finally, we can verify that

$$T_u^{\eta\text{-opt}}(B_{0,u}, R_{0,u}^S, F_{0,u}) = \frac{D_u}{B_{0,u} r_u} = \frac{D_u}{B_{1,u} r_u}. \quad (95)$$

Then select all elements from $(\mathbf{B}_0, \mathbf{R}_0^S, \mathbf{F}_0)$ that satisfy

$$\begin{aligned} R_{0,u}^S \leq B_{0,u} r_u < \frac{R_{0,u}^S}{\zeta_u}, \\ \frac{F_{0,u}}{\rho_u} < \frac{B_{0,u} r_u - R_{0,u}^S}{1 - \zeta_u}, \end{aligned} \quad (96)$$

or

$$B_{0,u} r_u \geq \frac{R_{0,u}^S}{\zeta_u}, \quad \frac{F_{0,u}}{\rho_u} < \frac{R_{0,u}^S}{\zeta_u}, \quad (97)$$

corresponding to the second and fourth row of Table I. For any one of those elements $(B_{0,u}, R_{0,u}^S, F_{0,u})$, we present a corresponding solution $(B_{1,u}, R_{1,u}^S, F_{1,u})$ which satisfies

$$\begin{cases} B_{1,u} = \frac{1}{r_u} \left(R_{0,u}^S + \frac{(1 - \zeta_u) F_{0,u}}{\rho_u} \right) & (98a) \\ R_{1,u}^S = R_{0,u}^S & (98b) \\ F_{1,u} = F_{0,u} & (98c) \end{cases}$$

We can first verify that

$$(B_{1,u}, R_{1,u}^S, F_{1,u}) \leq (B_{0,u}, R_{0,u}^S, F_{0,u}) \quad (99)$$

holds. Besides, we can verify that

$$R_{1,u}^S \leq B_{1,u}r_u \leq \frac{R_{1,u}^S}{\zeta_u} \quad (100)$$

and

$$\frac{F_{1,u}}{\rho_u} = \frac{B_{1,u}r_u - R_{1,u}^S}{1 - \zeta_u} \quad (101)$$

also hold. Finally, we can verify that

$$\begin{aligned} T_u^{\eta\text{-opt}}(B_{0,u}, R_{0,u}^S, F_{0,u}) &= \frac{D_u \rho_u}{F_{0,u}(1 - \zeta_u) + \rho_u R_{0,u}^S} \\ &= \frac{D_u \rho_u}{F_{1,u}(1 - \zeta_u) + \rho_u R_{1,u}^S} = \frac{D_u}{B_{1,u}r_u}. \end{aligned} \quad (102)$$

Next select all elements from $(\mathbf{B}_0, \mathbf{R}_0^S, \mathbf{F}_0)$ that satisfy

$$\begin{aligned} R_{0,u}^S \leq B_{0,u}r_u < \frac{R_{0,u}^S}{\zeta_u}, \\ \frac{F_{0,u}}{\rho_u} > \frac{B_{0,u}r_u - R_{0,u}^S}{1 - \zeta_u}, \end{aligned} \quad (103)$$

corresponding to the third row of Table I. For any one of those elements $(B_{0,u}, R_{0,u}^S, F_{0,u})$, we present a corresponding solution $(B_{1,u}, R_{1,u}^S, F_{1,u})$ which satisfies

$$\begin{cases} B_{1,u} = B_{0,u} & (104a) \\ R_{1,u}^S = R_{0,u}^S & (104b) \\ F_{1,u} = \rho_u \frac{B_{0,u}r_u - R_{0,u}^S}{1 - \zeta_u} & (104c) \end{cases}$$

We can first verify that

$$(B_{1,u}, R_{1,u}^S, F_{1,u}) \leq (B_{0,u}, R_{0,u}^S, F_{0,u}) \quad (105)$$

holds. Besides, we can verify that

$$R_{1,u}^S \leq B_{1,u}r_u \leq \frac{R_{1,u}^S}{\zeta_u} \quad (106)$$

and

$$\frac{F_{1,u}}{\rho_u} = \frac{B_{1,u}r_u - R_{1,u}^S}{1 - \zeta_u} \quad (107)$$

also hold. Finally, we can verify that

$$T_u^{\eta\text{-opt}}(B_{0,u}, R_{0,u}^S, F_{0,u}) = \frac{D_u}{B_{0,u}r_u} = \frac{D_u}{B_{1,u}r_u}. \quad (108)$$

Finally select all elements from $(\mathbf{B}_0, \mathbf{R}_0^S, \mathbf{F}_0)$ that satisfy

$$B_{0,u}r_u \geq \frac{R_{0,u}^S}{\zeta_u}, \quad \frac{F_{0,u}}{\rho_u} \geq \frac{R_{0,u}^S}{\zeta_u}, \quad (109)$$

corresponding to the fifth and sixth row of Table I. For any one of those elements $(B_{0,u}, R_{0,u}^S, F_{0,u})$, we present a corresponding solution $(B_{1,u}, R_{1,u}^S, F_{1,u})$ which satisfies

$$\begin{cases} B_{1,u} = \frac{R_{0,u}^S}{\zeta_u r_u} & (110a) \\ R_{1,u}^S = R_{0,u}^S & (110b) \\ F_{1,u} = \rho_u \frac{R_{0,u}^S}{\zeta_u} & (110c) \end{cases}$$

We can first verify that

$$(B_{1,u}, R_{1,u}^S, F_{1,u}) \leq (B_{0,u}, R_{0,u}^S, F_{0,u}) \quad (111)$$

holds. Besides, we can verify that

$$R_{1,u}^S \leq B_{1,u}r_u \leq \frac{R_{1,u}^S}{\zeta_u} \quad (112)$$

and

$$\frac{F_{1,u}}{\rho_u} = \frac{B_{1,u}r_u - R_{1,u}^S}{1 - \zeta_u} \quad (113)$$

also hold. Finally, we can verify that

$$\begin{aligned} T_u^{\eta\text{-opt}}(B_{0,u}, R_{0,u}^S, F_{0,u}) &= \frac{\zeta_u D_u}{R_{0,u}^S} \\ &= \frac{\zeta_u D_u}{R_{1,u}^S} = \frac{D_u}{B_{1,u}r_u}. \end{aligned} \quad (114)$$

Therefore, we could obtain a solution $(\mathbf{B}_1, \mathbf{R}_1^S, \mathbf{F}_1)$. From the above analysis we know that

$$(\mathbf{B}_1, \mathbf{R}_1^S, \mathbf{F}_1) \leq (\mathbf{B}_0, \mathbf{R}_0^S, \mathbf{F}_0), \quad (115)$$

which means that the solution $(\mathbf{B}_1, \mathbf{R}_1^S, \mathbf{F}_1)$ satisfy constraints (11b)-(11d) since $(\mathbf{B}_0, \mathbf{R}_0^S, \mathbf{F}_0)$ satisfy (8c)-(8e). Besides, from the above analysis, the solution $(\mathbf{B}_1, \mathbf{R}_1^S, \mathbf{F}_1)$ also satisfy constraints (11e) and (11f), and it could be easily verified that $(\mathbf{B}_1, \mathbf{R}_1^S, \mathbf{F}_1)$ also satisfy (11g)-(11i). Therefore, $(\mathbf{B}_1, \mathbf{R}_1^S, \mathbf{F}_1)$ is a feasible solution of problem (11).

From the above analysis, we also know that

$$\max_u T_u^{\eta\text{-opt}}(B_{0,u}, R_{0,u}^S, F_{0,u}) = \max_u \frac{D_u}{B_{1,u}r_u} \quad (116)$$

which causes contradiction to the original assumption. Thus, the assumption does not hold and the theorem is proved.

APPENDIX D PROOF OF Theorem 5

To prove the theorem, we first consider a new optimization problem

$$\min_{\mathbf{B}, \mathbf{R}^S, T} T \quad (117a)$$

$$\text{s.t. } T \geq \frac{D_u}{B_u r_u}, \quad \forall u = 1, \dots, U, \quad (117b)$$

$$\sum_{u=1}^U B_u \leq B_{\text{total}}, \quad (117c)$$

$$\sum_{u=1}^U R_u^S \leq R_{\text{total}}^S, \quad (117d)$$

$$R_u^S \leq B_u r_u \leq \frac{R_u^S}{\zeta_u}, \quad \forall u = 1, \dots, U, \quad (117e)$$

$$T \geq 0, \quad (117f)$$

$$B_u \geq 0, \quad \forall u = 1, \dots, U, \quad (117g)$$

$$R_u^S \geq 0, \quad \forall u = 1, \dots, U. \quad (117h)$$

We can see that problem (117) is obtained by removing the constraint (12e) from problem (12). For this problem, there is at least one set of optimal variables $(\mathbf{B}_0, \mathbf{R}_0^S, T_0)$ that satisfies

$$T_0 = \frac{D_u}{B_{0,u}r_u}, \quad \forall u = 1, \dots, U. \quad (118)$$

The reason is that if there exists a set of optimal variables $(\mathbf{B}_1, \mathbf{R}_1^S, T_1)$ that does not satisfy this condition, we could generate a new set of variable values as follows

$$\begin{cases} B_{0,u} = \frac{D_u}{T_1 r_u}, \forall u = 1, \dots, U, & (119a) \\ R_{0,u}^S = \frac{R_{1,u}^S}{B_{1,u}} \cdot \frac{D_u}{T_1 r_u}, \forall u = 1, \dots, U, & (119b) \\ T_0 = T_1. & (119c) \end{cases}$$

It can be easily verified that this solution satisfies (118). Since $T_0 = T_1$, this set of variable values is also optimal. Therefore, the following optimization problem has the same optimal objective function value as problem (117).

$$\min_{\mathbf{R}^S, T} T \quad (120a)$$

$$\text{s.t.} \quad \sum_{u=1}^U \frac{D_u}{r_u T} \leq B_{\text{total}}, \quad (120b)$$

$$\sum_{u=1}^U R_u^S \leq R_{\text{total}}^S, \quad (120c)$$

$$\zeta_u \frac{D_u}{T} \leq R_u^S \leq \frac{D_u}{T}, \quad \forall u = 1, \dots, U, \quad (120d)$$

$$T \geq 0, \quad (120e)$$

$$R_u^S \geq 0, \quad \forall u = 1, \dots, U. \quad (120f)$$

We could introduce a set of medium variables $\omega = [\omega_1, \dots, \omega_u, \dots, \omega_U]$ that satisfies

$$R_u^S = \omega_u \frac{D_u}{T}, \quad (121)$$

and problem (120) can be equivalently transformed into the following optimization problem

$$\min_{\omega, T} T \quad (122a)$$

$$\text{s.t.} \quad T \geq \frac{1}{B_{\text{total}}} \sum_{u=1}^U \frac{D_u}{r_u}, \quad (122b)$$

$$T \geq \frac{1}{R_{\text{total}}^S} \sum_{u=1}^U \omega_u D_u, \quad (122c)$$

$$T \geq 0, \quad (122d)$$

$$\zeta_u \leq \omega_u \leq 1, \quad \forall u = 1, \dots, U. \quad (122e)$$

We could easily obtain the optimal solution to this problem, which could be given by

$$\omega_u = \zeta_u, \quad \forall u = 1, \dots, U, \quad (123)$$

$$T = \max \left\{ \frac{\sum_{u=1}^U \frac{D_u}{r_u}}{B_{\text{total}}}, \frac{\sum_{u=1}^U \omega_u D_u}{R_{\text{total}}^S} \right\}. \quad (124)$$

Therefore, by substituting the medium variables ω , we can obtain a set of optimal variables to problem (117) written as follows

$$\bar{B}_u = \frac{D_u}{r_u} \min \left\{ \frac{B_{\text{total}}}{\sum_{u=1}^U \frac{D_u}{r_u}}, \frac{R_{\text{total}}^S}{\sum_{u=1}^U \zeta_u D_u} \right\}, \quad \forall u = 1, \dots, U, \quad (125)$$

$$\bar{R}_u^S = \zeta_u D_u \min \left\{ \frac{B_{\text{total}}}{\sum_{u=1}^U \frac{D_u}{r_u}}, \frac{R_{\text{total}}^S}{\sum_{u=1}^U \zeta_u D_u} \right\}, \quad \forall u = 1, \dots, U, \quad (126)$$

$$\bar{T} = \max \left\{ \frac{\sum_{u=1}^U \frac{D_u}{r_u}}{B_{\text{total}}}, \frac{\sum_{u=1}^U \zeta_u D_u}{R_{\text{total}}^S} \right\}. \quad (127)$$

Moreover, since that the inequality (18) holds, we can verify that the above solution also ensures constraint (12e) always holds. Since problem (117) is obtained by removing the constraint (12e) from problem (12), the above solution is also an optimal solution for problem (12), which proves the theorem.

REFERENCES

- [1] M. Erdelj, E. Natalizio, K. R. Chowdhury, and I. F. Akyildiz, "Help from the sky: Leveraging UAVs for disaster management," *IEEE Pervasive Comput.*, vol. 16, no. 1, pp. 24-32, Jan.-Mar. 2017.
- [2] I. Benkhelifa, N. Nouali-Taboudjemmat, and S. Moussaoui, "Disaster management projects using wireless sensor networks: An overview," in *Proc. Int. Conf. Adv. Inf. Networking Appl. Workshops (WAINA)*, Victoria, BC, Canada, 2014, pp. 605-610.
- [3] W. Feng, Y. Lin, Y. Wang, *et al.*, "Radio map-based cognitive satellite-UAV networks towards 6G on-demand coverage," *IEEE Trans. Cogn. Commun. Netw.*, early access, 2023.
- [4] F. Rinaldi, H. L. Maattanen, J. Torsner, *et al.*, "Non-terrestrial networks in 5G & beyond: A survey," *IEEE Access*, vol. 8, pp. 165178-165200, 2020.
- [5] W. Feng, Y. Wang, Y. Chen, N. Ge, and C.-X. Wang, "Structured satellite-UAV-terrestrial networks for 6G Internet of Things," *IEEE Netw.*, early access, 2024.
- [6] O. Kodheli, E. Lagunas, N. Maturo, *et al.*, "Satellite communications in the new space era: A survey and future challenges," *IEEE Commun. Surveys Tuts.*, vol. 23, no. 1, pp. 70-109, Firstquart. 2021.
- [7] N. Cheng, F. Lyu, W. Quan, *et al.*, "Space/aerial-assisted computing offloading for IoT applications: A learning-based approach," *IEEE J. Sel. Areas Commun.*, vol. 37, no. 5, pp. 1117-1129, May 2019.
- [8] GPRS; Overall Description of the GPRS Radio Interface; Stage 2 (Release 15); Revision 15.3.0, document TSG RAN WG3Meeting #43.064, 3GPP, Gothenburg, Sweden, Mar. 2020.
- [9] E-UTRA and E-UTRAN; Overall Description; Stage 2; Revision 16.1.0, document TSG RAN WG3Meeting #36.300, 3GPP, Gothenburg, Sweden, Apr. 2020.
- [10] U. Raza, P. Kulkarni, and M. Sooriyabandara, "Low Power Wide Area Networks: an overview," *IEEE Commun. Surveys Tuts.*, vol. 19, no. 2, pp. 855-873, Secondquart. 2017.
- [11] M. Centenaro, L. Vangelista, A. Zanella, and M. Zorzi, "Long-range communications in unlicensed bands: the rising stars in the IoT and smart city scenarios," *IEEE Wireless Commun.*, vol. 23, no. 5, pp. 60-67, Oct. 2016.
- [12] M. De Sanctis, E. Cianca, G. Araniti, I. Bisio, and R. Prasad, "Satellite communications supporting Internet of Remote Things," *IEEE Internet Things J.*, vol. 3, no. 1, pp. 113-123, Feb. 2016.
- [13] M. Centenaro, C. E. Costa, F. Granelli, C. Sacchi, and L. Vangelista, "A survey on technologies, standards and open challenges in satellite IoT," *IEEE Commun. Surveys Tuts.*, vol. 23, no. 3, pp. 1693-1720, Thirdquart. 2021.
- [14] X. Fang, W. Feng, T. Wei, Y. Chen, N. Ge, and C.-X. Wang, "5G embraces satellites for 6G ubiquitous IoT: Basic models for integrated satellite terrestrial networks," *IEEE Internet Things J.*, vol. 8, no. 18, pp. 14399-14417, Sep. 2021.

- [15] M. Bacco, L. Boero, P. Cassara, *et al.*, "IoT applications and services in space information networks," *IEEE Wireless Commun.*, vol. 26, no. 2, pp. 31-37, Apr. 2019.
- [16] Y. Zhu, W. Bai, M. Sheng, J. Li, D. Zhou, and Z. Han, "Joint UAV access and GEO satellite backhaul in IoRT networks: Performance analysis and optimization," *IEEE Internet Things J.*, vol. 8, no. 9, pp. 7126-7139, May 2021.
- [17] T. Ma, H. Zhou, B. Qian, *et al.*, "UAV-LEO integrated backbone: A ubiquitous data collection approach for B5G Internet of Remote Things networks," *IEEE J. Sel. Areas Commun.*, vol. 39, no. 11, pp. 3491-3505, Nov. 2021.
- [18] C. Liu, W. Feng, Y. Chen, C.-X. Wang, and N. Ge, "Cell-free satellite-UAV networks for 6G wide-area Internet of Things," *IEEE J. Sel. Areas Commun.*, vol. 39, no. 4, pp. 1116-1131, Apr. 2021.
- [19] Y. Wang, Z. Li, Y. Chen, *et al.*, "Joint resource allocation and UAV trajectory optimization for space-air-ground Internet of Remote Things networks," *IEEE Syst. J.*, vol. 15, no. 4, pp. 4745-4755, Dec. 2021.
- [20] Y. Lin, W. Feng, T. Zhou, *et al.*, "Integrating satellites and mobile edge computing for 6G wide-area edge intelligence: Minimal structures and systematic thinking," *IEEE Netw.*, vol. 37, no. 2, pp. 14-21, Mar./Apr. 2023.
- [21] D. Kim and S. Jeong, "Joint optimization of offloading scheduling and path planning for space-air-ground integrated edge computing systems," in *Proc. Int. Conf. ICT Convergence (ICTC)*, Jeju Island, Korea, Republic of, 2022, pp. 230-232.
- [22] N. N. Ei, J. S. Yoon, and C. S. Hong, "Energy-aware task offloading and resource allocation in space-aerial-integrated MEC system," in *Proc. Asia-Pacific Netw. Oper. Manag. Symp. (APNOMS)*, Takamatsu, Japan, 2022, pp. 1-6.
- [23] B. Chen, N. Li, Y. Li, X. Tao, and G. Sun, "Energy efficient hybrid offloading in space-air-ground integrated networks," in *Proc. IEEE Wireless Commun. Networking Conf. (WCNC)*, Austin, TX, USA, 2022, pp. 1319-1324.
- [24] Y. -H. Chao, C. -H. Chung, C. -H. Hsu, Y. Chiang, H. -Y. Wei, and C. -T. Chou, "Satellite-UAV-MEC collaborative architecture for task offloading in vehicular networks," in *Proc. IEEE Globecom Workshops (GC Wkshps)*, Taipei, Taiwan, 2020, pp. 1-6.
- [25] N. Waqar, S. A. Hassan, A. Mahmood, K. Dev, D. -T. Do, and M. Gidlund, "Computation offloading and resource allocation in MEC-enabled integrated aerial-terrestrial vehicular networks: A reinforcement learning approach," *IEEE Trans. Intell. Transp. Syst.*, vol. 23, no. 11, pp. 21478-21491, Nov. 2022.
- [26] C. Ding, J. -B. Wang, H. Zhang, M. Lin, and G. Y. Li, "Joint optimization of transmission and computation resources for satellite and high altitude platform assisted edge computing," *IEEE Trans. Wireless Commun.*, vol. 21, no. 2, pp. 1362-1377, Feb. 2022.
- [27] Z. Hu, F. Zeng, Z. Xiao, *et al.*, "Joint resources allocation and 3D trajectory optimization for UAV-enabled space-air-ground integrated networks," *IEEE Trans. Veh. Technol.*, vol. 72, no. 11, pp. 14214-14229, Nov. 2023.
- [28] F. Chai, Q. Zhang, H. Yao, X. Xin, R. Gao, and M. Guizani, "Joint multi-task offloading and resource allocation for mobile edge computing systems in satellite IoT," *IEEE Trans. Veh. Technol.*, vol. 72, no. 6, pp. 7783-7795, Jun. 2023.
- [29] C. Liu, W. Feng, X. Tao, and N. Ge, "MEC-empowered non-terrestrial network for 6G wide-area time-sensitive Internet of Things," *Engineering*, vol. 8, Jan. 2022, pp. 96-107.
- [30] A. Al-Hourani, S. Kandeepan, and S. Lardner, "Optimal LAP altitude for maximum coverage," *IEEE Wireless Commun. Lett.*, vol. 3, no. 6, pp. 569-572, Dec. 2014.
- [31] B. Wang, X. Li, D. Huang, and J. Xie, "A profit maximization strategy of MEC resource provider in the satellite-terrestrial double edge computing system," in *Proc. IEEE 21st International Conference on Communication Technology (ICCT)*, Tianjin, China, 2021, pp. 906-912.
- [32] J. Sharma, T. Choudhury, S. C. Satapathy, and A. S. Sabitha, "Study on H.265/HEVC against VP9 and H.264: on space and time complexity for codecs," in *Proc. International Conference on Communication, Computing and Internet of Things (IC3IoT)*, Chennai, India, 2018, pp. 106-110.
- [33] Y. Chen, W. Feng, and G. Zheng, "Optimum placement of UAV as relays," *IEEE Commun. Lett.*, vol. 22, no. 2, pp. 248-251, Feb. 2018.